

## IMPLICATION OF BARRIER FLUCTUATIONS ON THE RATE OF WEAKLY ADIABATIC ELECTRON TRANSFER

BARTŁOMIEJ DYBIEC\*, EWA GUDOWSKA-NOWAK† and PAWEŁ F. GÓRA‡

*M. Smoluchowski Institute of Physics, Jagellonian University  
ul. Reymonta 4, 30-059 Kraków, Poland*

*\*bartek@zfs.if.uj.edu.pl*

*†gudowska@th.if.uj.edu.pl*

*‡gora@if.uj.edu.pl*

The problem of escape of a Brownian particle in a cusp-shaped metastable potential is of special importance in nonadiabatic and weakly-adiabatic rate theory for electron transfer (ET) reactions. For the weakly-adiabatic reactions, the reaction follows an adiabaticity criterion in the presence of a sharp barrier. In contrast to the nonadiabatic case, the ET kinetics can be, however considerably influenced by the medium dynamics. In this paper, the problem of the escape time over a dichotomously fluctuating cusp barrier is discussed with its relevance to the high temperature ET reactions in condensed media.

*Keywords:* Kinetic rate; escape time; numerical evaluation of the resonant activation.

### 1. Introduction

Mechanism of the electron transfer (ET) in condensed and biological media goes beyond universal nonadiabatic approach of the Marcus theory.<sup>1–6</sup> In particular, relaxation properties of medium may slow down the overall ET kinetics and lead to an adiabatic dynamics.<sup>7</sup> An excess electron appearing in the medium introduces local fluctuations of polarization that in turn contribute to the change of Gibbs energy. Equilibration of those fluctuations leads to a new state with a localized position of a charge. In chemical reactions, the electron may change its location passing from a donating to an accepting molecule, giving rise to the same scenario of Gibbs energy changes that allow to discriminate between the (equilibrium) states “before” and “after” the transfer (see Fig. 1). The free energy surfaces for “reactants” and “products” are usually multidimensional functions which intersect at the transition point. The deviation from it, or the Gibbs energy change, can be calculated from the reversible work done along the path that forms that state, so that by using a simple thermodynamic argument, one is able to associate a change in the Gibbs energy with the change of multicomponent “reaction coordinate” that describes a response of the system to the instantaneous transfer of a charge from one site to another.

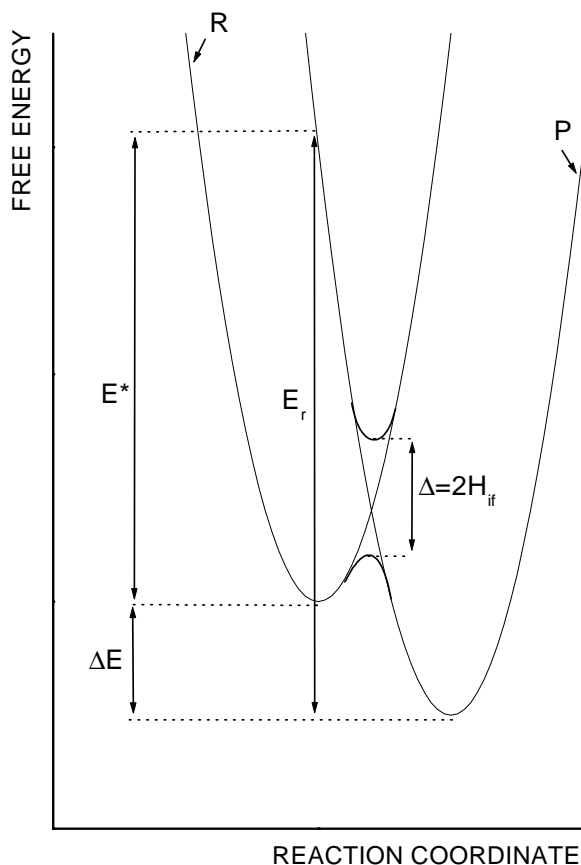


Fig. 1. Schematic energy profiles of reactant (**R**) and product (**P**) states of the electron transfer reaction coordinate. The reorganization energy  $E_r$  is the sum of the reaction energy  $\Delta E$  and the optical excitation energy  $E^*$ .  $\Delta$  stands for energy separation between the energy surfaces due to electronic coupling of **R** and **P** states. Thermal ET occurs at nuclear configurations characteristic to the intersection of the parabolas.

ET reactions involve both classical and quantum degrees of freedom. Quantum effects are mostly related to electronic degrees of freedom. Because of the mass difference between electrons and nuclei, it is frequently assumed that the electrons follow the nuclear motion adiabatically (Born–Oppenheimer approximation). The interaction between two different electronic states results in a splitting energy  $\Delta$ . The reaction from reactants to products is then mediated by an interplay of two parameters: time of charge fluctuations between the two neighboring electronic states and a typical time within which the nuclear reaction coordinate crosses the barrier region. When the electronic “uncertainty” time of charge fluctuations is shorter than the nuclear dynamics, the transition is adiabatic with the overall dynamics evolving on an adiabatic ground-state surface. For small splitting between electronic states  $\Delta \approx 0.1$ – $1$ , this ground-state adiabatic surface is often

characterized by a cusp-shaped potential.<sup>1,3,4,7</sup> In fact, it is often argued<sup>7</sup> that majority of natural ET reactions are in what we term weakly adiabatic regime, when the reaction is still adiabatic but the barrier is quite sharp and characterized by the barrier frequency  $\omega_a$  roughly by an order of magnitude higher than the medium relaxation frequency  $\omega_0$ .

The dynamics of the reaction coordinate in either of the potential wells can be estimated by use of a generalized Langevin equation with a friction term mimicking dielectric response of the medium. We are thus left with a standard model of a Brownian particle in a (generally time-dependent) medium.<sup>7,8</sup> In the case of a cusp-shaped potential, a particle approaching the top of a barrier with positive velocity will almost surely be pulled towards the other minimum. The kinetic rate is then determined<sup>7,9</sup> by the reciprocal mean first passage time (MFPT) to cross the barrier wall with positive velocity  $\dot{x} > 0$  and in a leading order in the barrier height  $\Delta E/k_B T$  yields the standard transition state theory (TST) result

$$k^{\text{cusp}} = \frac{\omega_0}{2\pi} \exp\left(-\frac{\Delta E}{k_B T}\right). \quad (1)$$

As discussed by Talkner and Braun,<sup>10</sup> the result holds also for non-Markovian processes with memory friction satisfying the fluctuation-dissipation theorem. The TST formula follows from the Kramers rate for the spatial-diffusion-controlled rate of escape at moderate and strong frictions  $\eta$

$$k_{R \rightarrow P} = \frac{(\eta^2/4 + \omega_a^2)^{1/2} - \eta/2}{\omega_a} \frac{\omega_0}{2\pi} \exp\left(-\frac{\Delta E}{k_B T}\right). \quad (2)$$

Here  $\omega_a$  stays for the positive-valued angular frequency of the unstable state at the barrier, and  $\omega_0$  is an angular frequency of the metastable state at  $x = R$ . For strong friction,  $\eta \gg \omega_a$  the above formula leads to a common Kramers result

$$k_{R \rightarrow P} = \frac{\omega_0 \omega_a}{2\pi \eta} \exp\left(-\frac{\Delta E}{k_B T}\right), \quad (3)$$

and reproduces the TST result, Eq. (1), after letting the barrier frequency tend to infinity  $\omega_a \rightarrow \infty$  with  $\eta$  held fixed. Moreover, as pointed out by Northrup and Hynes,<sup>8</sup> in a weakly adiabatic case, the barrier “point” is a negligible fraction of the high energy barrier region, so that the rate can be influenced by medium relaxation in the wells. The full rate constant for a symmetric reaction is then postulated in the form

$$k_{WA} = \left(1 + \frac{2k_{WA}^a}{k_D}\right)^{-1} k_{WA}^a, \quad (4)$$

where  $k_{WA}^a \approx k^{\text{cusp}}$  and  $k_D$  is the well (solvent or medium) relaxation rate constant which for a harmonic potential and a high barrier ( $\Delta E \geq 5k_B T$ ) within 10% of accuracy simplifies to

$$k_D = \frac{m_0 \omega_0^2 D}{k_B T} \left(\frac{\Delta E}{\pi k_B T}\right)^{1/2} e^{-\Delta E/k_B T}. \quad (5)$$

In the above equation, the diffusion constant  $D$  is related<sup>3</sup> *via* linear response theory to the longitudinal dielectric relaxation time  $\tau_L$  and for symmetric ET reaction ( $m_0^2\omega_0^2 = 2E_r$ ) reads

$$D = \frac{k_B T}{m_0 \omega_0^2 \tau_L} = \frac{k_B T}{2E_r \tau_L}. \quad (6)$$

Existence of a well defined rate constant for a chemical reaction requires that the relaxation time of all the degrees of freedom involved in the transformation, other than the reaction coordinate, is fast relative to motion along the reaction coordinate. If the separation of time scales were not present, the rate coefficient would have a significant frequency dependence reflecting various modes of relaxation. Such a situation can be expected in complex media, like non-Debye solvents or proteins, where there are many different types of degrees of freedom with different scales of relaxation. Although in these cases the rate “constant” can no longer be defined, the overall electron transfer can be described in terms of the mean escape time that takes into account noisy character of a potential surface along with thermal fluctuations.

The time effect of the surroundings (“environmental noise”), expressed by different time constants for polarization and the dielectric reorganization has not been so far explored in detail, except in photochemical reaction centers<sup>5</sup> where molecular dynamics studies have shown that the slow components of the energy gap fluctuations are, most likely, responsible for the observed nonexponential kinetics of the primary ET process. The latter will be assumed here to influence the activation free energy of the reaction  $\Delta E = E_r/4$  and will be envisioned as a barrier alternating processes. In consequence, even small variations  $\delta E$  in  $\Delta E$  can greatly modulate the escape kinetics (passage from reactants’ to products’ state) in the system. If the barrier fluctuates extremely slowly, the mean first passage time to the top of the barrier is dominated by those realizations for which the barrier starts in a higher position and thus becomes very long. The barrier is then essentially quasistatic throughout the process. At the other extreme, in the case of rapidly fluctuating barrier, the mean first passage time is determined by the “average barrier”. For some particular correlation time of the barrier fluctuations, it can happen however, that the mean kinetic rate of the process exhibits an extremum<sup>11–13</sup> that is a signature of resonant tuning of the system in response to the external noise.

In this contribution we present analytical and numerical results for the escape kinetics over a fluctuating cusp for the high temperature model ET system with a harmonic potential subject to dichotomous fluctuations. We perform our investigations of the average escape time as a function of the correlation rate of the dichotomous noise in the barrier height at fixed temperatures. In particular, we examine variability of the mean first passage time for different types of barrier switching<sup>11,14,15</sup> when the barrier changes either between the “on-off” position, flips between a barrier or a well, or it varies between two different heights. By using a Monte Carlo procedure we determine probability density function (pdf) of escape

time in the system and investigate the degree of nonexponential behavior in the decay of a primary state located in the reactants' well.

### 2. Generic Model System

At high temperatures it is permissible to treat the low frequency medium modes classically. The medium coordinates are continuous and it is useful to draw a one-dimensional schematic representation of the system (Fig. 1) with the reaction proceeding almost exclusively at the intersection energy. As a model of the reaction coordinate kinetics, we have considered an overdamped Brownian particle moving in a potential field between absorbing and reflecting boundaries in the presence of noise that modulates the barrier height. The evolution of the reaction coordinate  $x(t)$  is described in terms of the Langevin equation

$$\frac{dx}{dt} = -V'(x) + \sqrt{2T}\xi(t) + g(x)\eta(t) = -V'_\pm(x) + \sqrt{2T}\xi(t). \tag{7}$$

Here  $\xi(t)$  is a Gaussian process with zero mean and correlation  $\langle \xi(t)\xi(s) \rangle = \delta(t-s)$  (i.e., the Gaussian white noise arising from the heat bath of temperature  $T$ ),  $\eta(t)$  stands for a dichotomous (not necessarily symmetric) noise taking on one of two possible values  $a_\pm$  and prime means differentiation over  $x$ . Correlation time of the dichotomous process has been set up to  $1/(2\gamma)$  with  $\gamma$  expressing the flipping frequency of the barrier fluctuations. Both noise are assumed to be statistically independent, i.e.,  $\langle \xi(t)\eta(s) \rangle = 0$ . Equivalent to Eq. (7) is a set of the Fokker-Planck equations describing evolution of the probability density of finding the particle at time  $t$  at the position  $x$  subject to the force  $-V'_\pm(x) = -V'(x) + a_\pm g(x)$

$$\partial_t P(x, a_\pm, t) = \partial_x [V'_\pm(x) + T\partial_x]P(x, a_\pm, t) - \gamma P(x, a_\pm, t) + \gamma P(x, a_\mp, t). \tag{8}$$

In the above equations time has dimension of [length]<sup>2</sup>/energy due to a friction constant that has been “absorbed” in the time variable. We are assuming absorbing boundary condition at  $x = L$  and a reflecting boundary at  $x = 0$

$$P(L, a_\pm, t) = 0, \tag{9}$$

$$[V'_\pm(x) + T\partial_x]P(x, a_\pm, t)|_{x=0} = 0. \tag{10}$$

The initial condition

$$P(x, a_+, 0) = P(x, a_-, 0) = \frac{1}{2} \delta(x) \tag{11}$$

expresses equal choice to start with any of the two configurations of the barrier. The quantity of interest is the mean first passage time

$$\begin{aligned} \text{MFPT} &= \int_0^\infty dt \int_0^L [P(x, a_+, t) + P(x, a_-, t)] dx \\ &= \tau_+(0) + \tau_-(0) \end{aligned} \tag{12}$$

with  $\tau_+$  and  $\tau_-$  being MFPT for (+) and (-) configurations, respectively. MFPTs  $\tau_+$  and  $\tau_-$  fulfill the set of backward Kolmogorov equations<sup>13</sup>

$$-\frac{1}{2} = -\gamma\tau_{\pm}(x) + \gamma\tau_{\mp}(x) - \frac{dV_{\pm}(x)}{dx} \frac{d\tau_{\pm}(x)}{dx} + T \frac{d^2\tau_{\pm}(x)}{dx^2} \tag{13}$$

with the boundary conditions [cf. Eqs. (9) and (10)]

$$\tau'_{\pm}(x)|_{x=0} = 0, \quad \tau_{\pm}(x)|_{x=L} = 0. \tag{14}$$

Although the solution of Eq. (13) is usually unique,<sup>16</sup> a closed, “ready to use” analytical formula for the MFPT can be obtained only for the simplest cases of the potentials (piecewise linear). More complex cases, like even piecewise parabolic potential  $V_{\pm}$  result in an intricate form of the solution to Eq. (13). Other situations require either the use of approximation schemes,<sup>17</sup> perturbative approach<sup>12</sup> or direct numerical evaluation methods.<sup>18,19</sup> In order to examine MFPT for various potentials a modified program<sup>20</sup> applying general shooting methods has been used. Part of the mathematical software has been obtained from the *Netlib* library.

### 3. Solution and Results

Equivalent to Eq. (13) is a set of equations

$$\begin{aligned} \begin{bmatrix} \frac{du(x)}{dx} \\ \frac{dv(x)}{dx} \\ \frac{dp(x)}{dx} \\ \frac{dq(x)}{dx} \end{bmatrix} &= \begin{bmatrix} 0 & 0 & 1 & 0 \\ 0 & 0 & 0 & 1 \\ 0 & 0 & \frac{(d/dx)[V_+(x) + V_-(x)]}{2T} & \frac{(d/dx)[V_+(x) - V_-(x)]}{2T} \\ 0 & \frac{2\gamma}{T} & \frac{(d/dx)[V_+(x) - V_-(x)]}{2T} & \frac{(d/dx)[V_+(x) + V_-(x)]}{2T} \end{bmatrix} \\ &\times \begin{bmatrix} u(x) \\ v(x) \\ p(x) \\ q(x) \end{bmatrix} + \begin{bmatrix} 0 \\ 0 \\ -\frac{1}{T} \\ 0 \end{bmatrix}, \end{aligned} \tag{15}$$

where new variables have been introduced

$$\begin{cases} u(x) = \tau_+(x) + \tau_-(x) \\ v(x) = \tau_+(x) - \tau_-(x) \end{cases}, \quad \begin{cases} \frac{du(x)}{dx} = p(x) \\ \frac{dv(x)}{dx} = q(x) \end{cases}. \tag{16}$$

Since  $u$  does not enter the right-hand side of any of the above equations, the system can be further converted to

$$\begin{aligned} \begin{bmatrix} \frac{dv(x)}{dx} \\ \frac{dp(x)}{dx} \\ \frac{dq(x)}{dx} \end{bmatrix} &= \begin{bmatrix} 0 & 0 & 1 \\ 0 & \frac{(d/dx)[V_+(x) + V_-(x)]}{2T} & \frac{(d/dx)[V_+(x) - V_-(x)]}{2T} \\ \frac{2\gamma}{T} & \frac{(d/dx)[V_+(x) - V_-(x)]}{2T} & \frac{(d/dx)[V_+(x) + V_-(x)]}{2T} \end{bmatrix} \\ &\times \begin{bmatrix} v(x) \\ p(x) \\ q(x) \end{bmatrix} + \begin{bmatrix} 0 \\ -\frac{1}{T} \\ 0 \end{bmatrix} \end{aligned} \tag{17}$$

i.e., it has a form of

$$\frac{d\mathbf{f}(x)}{dx} = \hat{A}(x)\mathbf{f}(x) + \boldsymbol{\beta}(x). \tag{18}$$

A unique solution to Eq. (18) exists<sup>16</sup> and reads

$$\begin{aligned} \mathbf{f}(x) &= \exp\left\{\int_0^x \hat{A}(x')dx'\right\} \mathbf{f}(0) \\ &+ \exp\left\{\int_0^x \hat{A}(x')dx'\right\} \int_0^x \exp\left\{-\int_0^{x'} \hat{A}(x'')dx''\right\} \boldsymbol{\beta}(x')dx' \\ &= \mathbf{A}(x)\mathbf{f}(0) + \mathbf{A}(x)\mathbf{B}(x) = \mathbf{A}(x)\mathbf{f}(0) + \mathbf{C}(x) \end{aligned} \tag{19}$$

with boundary conditions leading to

$$\mathbf{f}(0) = \begin{bmatrix} \tau_+ - \tau_- \\ 0 \\ 0 \end{bmatrix}, \quad \mathbf{f}(L) = \begin{bmatrix} 0 \\ p(L) \\ q(L) \end{bmatrix}. \tag{20}$$

MFPT is the quantity of interest

$$\tau = \tau(0) = u(0), \tag{21}$$

which can be obtained from

$$p(x) = \frac{du(x)}{dx}, \tag{22}$$

and

$$\int_0^L p(x)dx = u(L) - u(0) = 0 - u(0) = -u(0), \tag{23}$$

with

$$u(0) = \tau = -\int_0^L p(x)dx. \tag{24}$$

For the parabolic potential  $V_+(x) = -V_-(x) = Hx^2/L^2 \equiv 2E_r x^2$  the above procedure leads to

$$\hat{A}(x) = \begin{bmatrix} 0 & 0 & 1 \\ 0 & 0 & \frac{2Hx}{L^2T} \\ \frac{2\gamma}{T} & \frac{2Hx}{L^2T} & 0 \end{bmatrix}, \quad \int_0^x \hat{A}(x)dx = x \begin{bmatrix} 0 & 0 & 1 \\ 0 & 0 & \frac{Hx}{L^2T} \\ \frac{2\gamma}{T} & \frac{Hx}{L^2T} & 0 \end{bmatrix}, \quad (25)$$

and

$$\tau = \int_0^L \int_0^L \Phi(x, y) dx dy, \quad (26)$$

where

$$\begin{aligned} \Phi(x, y) = & \left[ -\frac{L^2 H x [\varphi(x) - 2]}{2} \frac{1}{\rho(x)} - \frac{LH[\varphi(L) - 2]}{4[H^2 + \gamma T L^2 \varphi(L)]} \frac{4\gamma L^4 T + H^2 x^2 \varphi(x)}{\rho(x)} \right. \\ & \left. + \frac{\sqrt{\rho(L)} \xi(L) H}{4[H^2 + \gamma T L^2 \varphi(L)]} \frac{x \xi(x)}{\sqrt{\rho(x)}} \right] \times H \gamma L^2 \frac{y[\varphi(y) - 2]}{\rho(y)} \\ & + \left[ \frac{H^2 L^4 \gamma y [\varphi(y) - 2]}{2\rho(y)} \frac{x[\varphi(x) - 2]}{\rho(x)} - \frac{H^2 y \xi(y)}{4T \sqrt{\rho(y)}} \frac{x \xi(x)}{\sqrt{\rho(x)}} \right. \\ & \left. + \frac{4\gamma L^4 T + H^2 y^2 \varphi(y)}{4T \rho(y)} \frac{4\gamma L^4 T + H^2 x^2 \varphi(x)}{\rho(x)} \right] \times \theta(y - x), \end{aligned} \quad (27)$$

$$\rho(x) = H^2 x^2 + 2\gamma L^4 T, \quad (28)$$

$$\varphi(x) = \exp \left[ \frac{\sqrt{\rho(x)} x}{L^2 T} \right] + \exp \left[ \frac{-\sqrt{\rho(x)} x}{L^2 T} \right] = 2 \cosh \left[ \frac{\sqrt{\rho(x)} x}{L^2 T} \right], \quad (29)$$

$$\xi(x) = \exp \left[ \frac{\sqrt{\rho(x)} x}{L^2 T} \right] - \exp \left[ \frac{-\sqrt{\rho(x)} x}{L^2 T} \right] = 2 \sinh \left[ \frac{\sqrt{\rho(x)} x}{L^2 T} \right]. \quad (30)$$

Figure 2 displays calculated MFPT as a function of switching frequency  $\gamma$ . Analytical solutions are presented along with results from Monte Carlo simulations of Eq. (7). As a choice for various configurations of the potential, we have probed  $H_{\pm} = \pm 8T$ ;  $H_+ = 8T$ ,  $H_- = 0$  and  $H_+ = 8T$ ,  $H_- = 4T$  that set up reorganization energies ( $2E_r = H$ ) and heights of barrier in the problem of interest.

The distinctive characteristics of resonant activation is observed with the average escape time initially decreasing, reaching a minimum value, and then increasing as a function of switching frequency  $\gamma$ . At slow dynamics of the barrier height, i.e., for values of the rate  $\gamma$  less than  $\tau_+^{-1}$ , the average escape time approaches the value  $\tau = (\tau_- - \tau_+)/2$  predicted by theory<sup>11,15,17,21</sup> and observed in experimental investigations of resonant activation.<sup>22</sup> For fast dynamics of the barrier height the average escape time reaches the value associated with an effective potential characterized



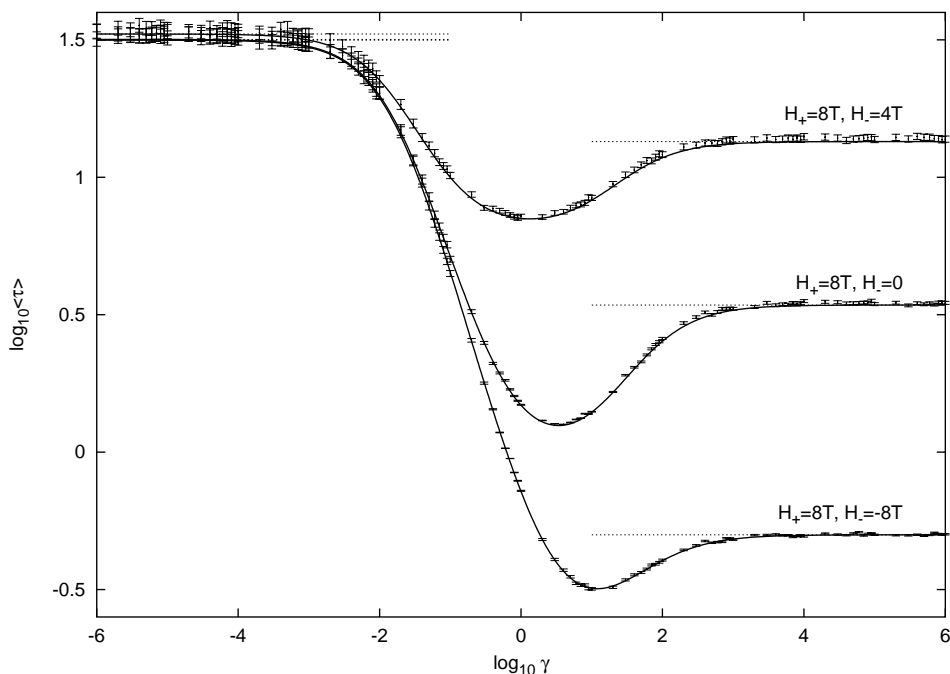


Fig. 2. MFPT as a function of the correlation rate of the dichotomous noise for parabolic potential barriers switching between different heights  $H_{\pm}$ . Full lines: analytical results; symbols stay for the results from MC simulations with  $\Delta t = 10^{-5}$  and ensemble of  $N = 10^4$  trajectories. For simplicity, the parametrization  $L = T = 1$  has been used.

by an average barrier. In comparison to the “on-off” switching of the barrier, the region of resonant activation flattens for dichotomic flipping between the barrier and a well, and in the case of the Bier–Astumian model ( $H_+ = 8T, H_- = 4T$ ) when the barrier changes its height between two different values. The resonant frequency shifts from the lowest value for the Bier–Astumian model to higher values for the “on-off” and the “barrier-well” scenarios, respectively. This observation is in agreement with former studies<sup>15</sup> aimed to discriminate between characteristic features of resonant activation for models with “up-down” configurations of the barrier and models with the “up” configuration but fluctuating between different heights. The “up-down” switching of the barrier heights produces shorter MFPT and in consequence, higher value of crossing rates for resonant frequencies than two other models of barrier switching.

For each of the above situations we have evaluated probability density function for first escape times. Pdfs have been obtained as a result of MC simulations on  $N = 10^4$  trajectories by using histograms and kernel density estimation methods. In the resonant activation regime, pdf of escape times has an exponential slope that suggests the reactants’ population follows preferentially the kinetics through the state with the lowest barrier. Similarly, the exponential decay times of reactants’

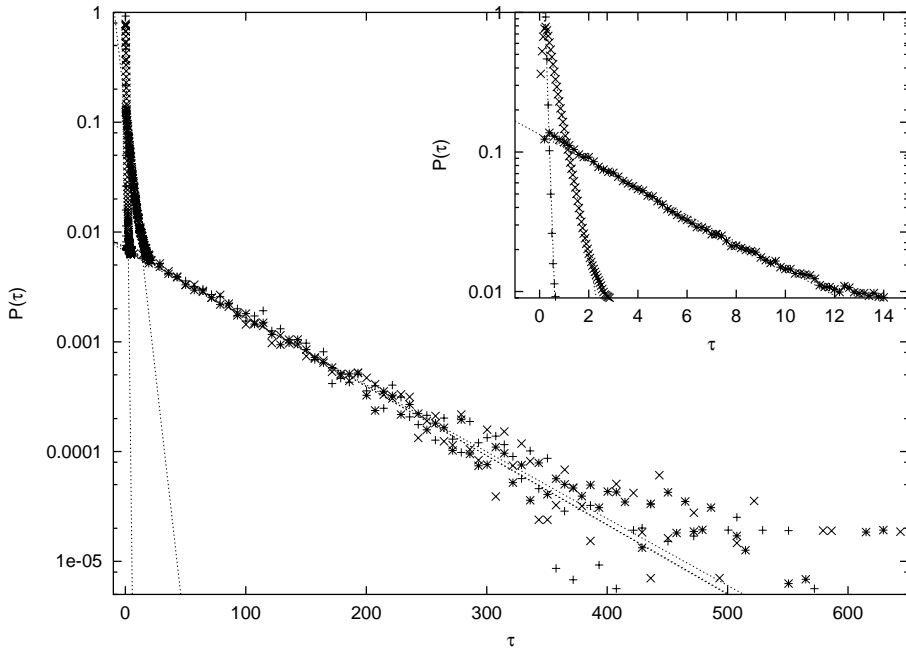


Fig. 3. Semilog plot of the pdf for first escape times in the system. The differences between lines fitted to the slopes reflect various  $\tau_-$  values for a given type of barrier switching: (+) for  $H_+ = 8T$ ,  $H_- = -8T$ ; (x) for  $H_+ = 8T$ ,  $H_- = 0$  and (\*) for  $H_+ = 8T$ ,  $H_- = 4T$  (cf. Table 1).

are observed in the high frequency limit ( $\gamma \approx 10^9$ ), when the system experiences an effective potential with an average barrier.<sup>11,14,15,17,19,22–24</sup>

Apparent nonexponential decay of the initial population is observed at low frequencies ( $\gamma \approx 10^{-6}$ ), when the flipping rate becomes less than  $\tau_-^{-1}$ . As it is clearly demonstrated in Fig. 3 and summarized in Table 1, passage times at low frequencies are roughly characterized by two distinct time scales that correspond to  $\tau_-$  (different for various switching barrier scenarios — cf. first three rows of Table 1) and  $\tau_+$  (bottom three rows of Table 1), respectively. The inset of Fig. 3 shows pdf zoomed for part of the main plot, where the differences between various, model dependent  $\tau_-$  values can be well distinguished.

Table 1. Relaxation time for parabolic potential barriers switching between different heights  $H_{\pm}$  at low frequencies.

	$H_+$	$H_-$	Fitted value	Static barrier value
$\tau_-$	8T	-8T	$0.09 \pm 0.01$	0.12
	8T	0	$0.46 \pm 0.01$	0.50
	8T	4T	$4.51 \pm 0.05$	3.43
$\tau_+$	8T	-8T	$68.73 \pm 0.89$	63.01
	8T	0	$71.33 \pm 3.04$	63.01
	8T	4T	$79.11 \pm 1.98$	63.01

#### 4. Summary

In the foregoing sections we have considered the thermally activated process that can describe classical ET kinetics. The regime of dynamical disorder where fluctuations of the environment can interplay with the time scale of the reaction itself is not so well understood. The examples where such a physical situation can happen are common to nonequilibrium chemistry and, in particular to ET reactions<sup>5</sup> in photosynthesis. As a toy model for describing the nonexponential ET kinetics<sup>5</sup> we have chosen a generic system displaying the resonant activation phenomenon. The reaction coordinate has been coupled to an external noise source that can describe polarization and depolarization processes responsible for the height of barrier between the reactants and products wells. We have assumed that the driving forces for the ET process interconvert at a rate  $\gamma$  reflecting dynamic changes in the transition state. The best tuning of the system and its highest ET rate can be achieved within the resonant frequency region. On the other hand, nonexponential ET kinetics can be attributed to long, time-persisting correlations in barrier configuration that effectively change a Poissonian character of escape events demonstrating, in general, multiscale time-decay of initial population.

#### Acknowledgments

This project has been partially supported by the Marian Smoluchowski Institute of Physics, Jagellonian University research grant (E. Gudowska-Nowak).

The contribution is Authors' dedication to the 50th birthday anniversary of Prof. Jerzy Luczka.

#### References

1. R. A. Marcus and N. Sutin, *Biochim. Biophys. Acta* **811**, 265 (1985).
2. R. A. Marcus, *J. Phys. Chem.* **98**, 7170 (1994).
3. J. Ulstrup, *Charge Transfer in Condensed Media* (Springer-Verlag, Berlin, 1979).
4. J. Jortner and M. Bixon (eds.), *Advances in Chemical Physics: Electron Transfer — From Isolated Molecules to Biomolecules*, Vol. 106 (Wiley, New York, 1999).
5. J. N. Gehlen, M. Marchi, and D. Chandler, *Science* **263**, 499 (1994).
6. N. Makri, E. Sim, D. E. Makarov, and M. Topaler, *Proc. Natl. Acad. Sci. USA* **93**, 3926 (1996).
7. J. T. Hynes, *J. Phys. Chem.* **90**, 3701 (1986).
8. S. H. Northrup and J. T. Hynes, *J. Chem. Phys.* **73**, 2700 (1980).
9. P. Hänggi, P. Talkner, and M. Borkovec, *Rev. Mod. Phys.* **62**, 251 (1990).
10. P. Talkner and H. B. Braun, *J. Chem. Phys.* **88**, 7357 (1988).
11. Ch. R. Doering and J. C. Gadoua, *Phys. Rev. Lett.* **69**, 2318 (1992).
12. J. Iwaniszewski, *Phys. Rev. E* **54**, 3173 (1996).
13. P. Pechukas and P. Hänggi, *Phys. Rev. Lett.* **73**, 2772 (1994).
14. U. Zürcher and Ch. R. Doering, *Phys. Rev. E* **47**, 3862 (1993).
15. M. Bögüná, J. M. Porrà, J. Masoliver, and K. Lindenberg, *Phys. Rev. E* **57**, 3990 (1998).
16. R. M. M. Mattheij and J. Molenaar, *Ordinary Differential Equations in Theory and Practice* (John Wiley and Sons, Chichester, 1996).

17. P. Reimann, R. Bartussek, and P. Hänggi, *Chem. Phys.* **235**, 11 (1998).
18. W. H. Press, S. A. Teucholsky, W. T. Vetterling, and B. F. Flannery, *Numerical Recipes. The Art of Scientific Computing* (Cambridge University Press, Cambridge, 1992).
19. L. Gammaitoni, P. Hänggi, P. Jung, and Marchesoni, *Rev. Mod. Phys.* **70**, 223 (1998).
20. R. M. M. Mattheij and G. W. M. Staarink, MUS.F program for solving general two point boundary problems (<http://www.netlib.org>).
21. D. Astumian and M. Bier, *Phys. Rev. Lett.* **72**, 1766 (1994).
22. R. N. Mantegna and B. Spagnolo, *Phys. Rev. Lett.* **84**, 3025 (2000).
23. P. Reimann and P. Hänggi, in *Stochastic Dynamics, Lecture Notes in Physics*, Vol. 484, eds. L. S. Geier and T. Pöschel (Springer-Verlag, Berlin, 1997), pp. 127–139.
24. B. Dybiec and E. Gudowska-Nowak, *Phys. Rev. E* **66**, 026123 (2002).

